Protein Science (1996), 5:2044–2053. Cambridge University Press. Printed in the USA.

Bending of the calmodulin central helix: A theoretical study

DAVID VAN DER SPOEL,[1] BERT L. DE GROOT,[1] STEVEN HAYWARD,[1]
HERMAN J.C. BERENDSEN,[1] AND HANS J. VOGEL[2]

[1] Department of Biophysical Chemistry, University of Groningen, Nijenborgh 4, 9747 AG Groningen, The Netherlands
[2] Department of Biological Sciences, University of Calgary, Calgary, Alberta T2N 1N4, Canada

(RECEIVED May 2, 1996; ACCEPTED July 22, 1996)

Abstract

The crystal structure of calcium–calmodulin (CaM) reveals a protein with a typical dumbbell structure. Various spectroscopic studies have suggested that the central linker region of CaM, which is α-helical in the crystal structure, is flexible in solution. In particular, NMR studies have indicated the presence of a flexible backbone between residues Lys 77 and Asp 80. This flexibility is related directly to the function of the protein because it enables the N- and C-terminal domains of the protein to move toward each other and bind to the CaM-binding domain of a target protein. We have investigated the flexibility of the CaM central helix by a variety of computational techniques: molecular dynamics (MD) simulations, normal mode analysis (NMA), and essential dynamics (ED) analysis. Our MD results reproduce the experimentally determined location of the bend in a simulation of only the CaM central helix, indicating that the bending point is an intrinsic property of the α-helix, for which the remainder of the protein is not important. Interestingly, the modes found by the ED analysis of the MD trajectory are very similar to the lowest frequency modes from the NM analysis and to modes found by an ED analysis of different structures in a set of NMR structures. Electrostatic interactions involving residues Arg 74 and Asp 80 seem to be important for these bending motions and unfolding, which is in line with pH-dependent NMR and CD studies.

Keywords: essential dynamics; molecular dynamics simulations; normal modes; protein folding; calmodulin

Calcium is an important secondary messenger in all eukaryotic cells. Specialized ATP-driven pumps secrete calcium to the extracellular environment, or into the intracellular storage organelles, creating a large calcium gradient over the membrane. During stimulation, the calcium can flow rapidly down the concentration gradient into the cytoplasmic space of a cell. A host of calcium-binding proteins is responsible for translating the sudden rise in the intracellular calcium concentration into a carefully orchestrated cellular response. A unique feature of these regulatory calcium-binding proteins is that they all comprise characteristic helix-loop-helix calcium binding sites (Finn & Forsen, 1995; Ikura, 1996). Calmodulin, a 148-residue acidic protein, appears to be the most versatile member of this family of proteins. It is present in all eukaryotic cells; in addition, it has been implicated in the activation of at least 30 different target proteins and enzymes (Vogel & Zhang, 1995; Ikura, 1996). Considering that most other calcium-regulatory proteins generally only activate one specific target, this promiscuity is one of the most interesting features of CaM. Consequently, research has focused on the molecular features that allow this protein to act efficiently on the CaM-binding domains of target proteins, which do not share significant amino acid homology.

The first distinct feature of CaM is its high Met content. The preponderance of Met in its target peptide binding sites is thought to create two highly pliable, yet sticky, surfaces, which can accommodate the binding of peptides with different amino acid sequences (Vogel, 1994; Zhang & Vogel, 1994). Second, CaM has a rather unconventional dumbbell structure, and the intrinsic flexibility of its central linker region allows a reorientation of the position of the two domains of CaM such that it can interact optimally with its target peptide. In the crystal structure of the Ca^{2+} form of the protein, this region appears as an extended α-helix. However, in solution, studies of the apo and Ca^{2+} form of the protein have shown that the central part of this region is flexible (Heidorn & Trewhella, 1988; Persechini & Kretsinger, 1988; Ikura et al., 1991; Spera et al., 1991; Barbato et al., 1992; Kuboniwa et al., 1995; Tjandra et al., 1995; Zhang et al., 1995). In complexes of CaM with target peptides, the α-helicity of the central helix decreases further (Spera et al., 1991; Ikura et al., 1992; Meador et al., 1992; Clore et al., 1993).

Reprint requests to: Hans J. Vogel, Department of Biological Sciences, University of Calgary, 2500 University Drive N.W., Calgary, Alberta T2N 1N4, Canada; e-mail: vogel@acs.ucalgary.ca.

Abbreviations: CaM, calmodulin; MLCK, myosin light chain kinase; MD, molecular dynamics; ED, essential dynamics; NMA, normal mode analysis; Sim. Pep, simulation of CaM central helix; Sim. Pro, simulation of intact CaM; RMSD, RMS deviation.

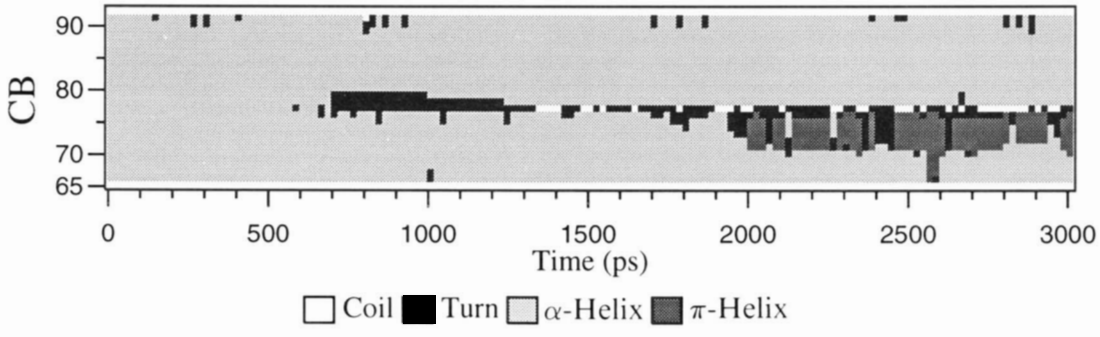

Fig. 1. Secondary structure of the CaM central helix as a function of simulation time.

The capacity of this region of CaM to adjust its secondary structure in response to the physiologic conditions is of considerable interest, and has prompted us to undertake molecular dynamics simulations of this part of the protein. Two earlier MD simulations have been reported for CaM; these were done over relatively short time periods (150 ps, Mehler et al., 1991; 600 ps, Vorherr et al., 1992) and in the absence of full solvent: in one study (Vorherr et al., 1992), artificial bends were introduced in the central linker region. In order to extend on these earlier studies, we have performed our simulations in a box containing explicit water molecules. We have done a 500-ps simulation of the entire protein (Sim. Pro), as well as a 3-ns simulation of the 28-residue isolated central helix (Sim. Pep). In this way, we can compare the dynamics of the CaM central helix in the protein with the isolated peptide to investigate whether the flexibility of the backbone of the CaM central helix is a property of the α-helix alone.

In general, peptide simulations do not reproduce equilibrium conditions. However, it is possible to study kinetic processes, like the unfolding of peptides (Soman et al., 1991; Daggett & Levitt, 1992; Brooks & Case, 1993; Caflisch & Karplus, 1994; Kazmirski et al., 1995; van der Spoel et al., 1996c). The majority of MD studies reported for isolated α-helices to date involved model peptides where no experimental benchmark is available, some notable exceptions being MD simulations of the ribonuclease S-peptide analogue (Tirado-Rives & Jorgensen, 1991) and the myoglobin H-helix (van Buuren & Berendsen, 1993; Hirst & Brooks, 1995). Although no published structural data for the excised central helix of CaM is available, we have assumed that we can compare our simulation results to the data for the protein crystals, at least at the beginning of the simulation; this approach allows us to test the stability of the central helix in aqueous solution. Finally, we will analyze the motions in the isolated CaM central helix to test whether intrinsic motions of the α-helical peptide are important for flexibility or unfolding of the peptide.

Results

The primary focus of this work is on the CaM central helix (Sim. Pep), therefore we will not present the simulation for the intact protein (Sim. Pro); this will only be mentioned where it is useful to compare the results of the two separate simulations.

Secondary structure

A very important analysis on structure of peptides and proteins, in our opinion, is a secondary structure analysis. We have used the DSSP program (Kabsch & Sander, 1983), which computes the secondary structure of each residue in a sequence from the atomic coordinates. Using a color code, it is possible to follow the secondary structure for each residue as a function of time. This is shown for Sim. Pep in Figure 1. From the trajectory, we have extracted a snapshot every 20 ps and these coordinates were used to compute the secondary structure. Little happens to the α-helix initially, but after 700 ps, residues Met 76–Thr 79 lose their α-helical structure. After 1,200 ps, only Lys 77 seems to be nonhelical, but after 1,900 ps, a larger portion of the α-helix, starting from Met 71, turns into a π-helix. This structure is then rather stable until the end of the simulation, except around 2,560 ps, when there is an 11-residue π-helix. The C-terminal end of the helix (starting at Asp 80) is stable throughout; only small fluctuations at the very end of the α-helix occur. We have plotted the time-average of the α-helicity per residue for both Sim. Pep and Sim. Pro in Figure 2, using the criterion of Hirst and Brooks (1995), which is based on ϕ/ψ angles. It is clear from this figure that the central residues are less α-helical in Sim. Pep. The CaM central helix in Sim. Pro is stable; it does not unfold at all under these conditions. What happens to the peptide is illustrated by some snapshots from the Sim. Pep trajectory (Fig. 3). The α-helix bends in the center, but it remains rather helical on both ends. However, it can be seen though, that the N terminus of the α-helix (left side in the figure) is somewhat swollen at 3,000 ps, corresponding to the larger radius associated with the π-helix structure type found by DSSP (Fig. 1).

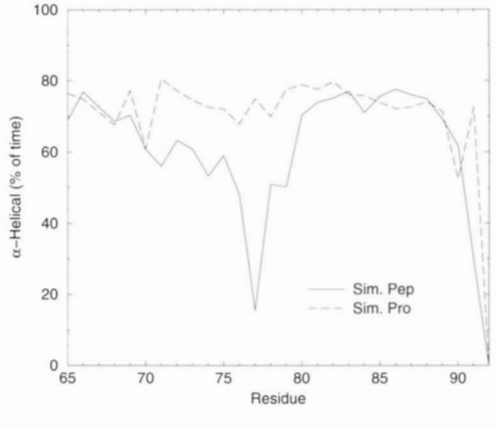

Fig. 2. Time-average of α-helicity per residue of the CaM central helix in Sim. Pep and Sim. Pro computed using the criterion of Hirst and Brooks (1995).

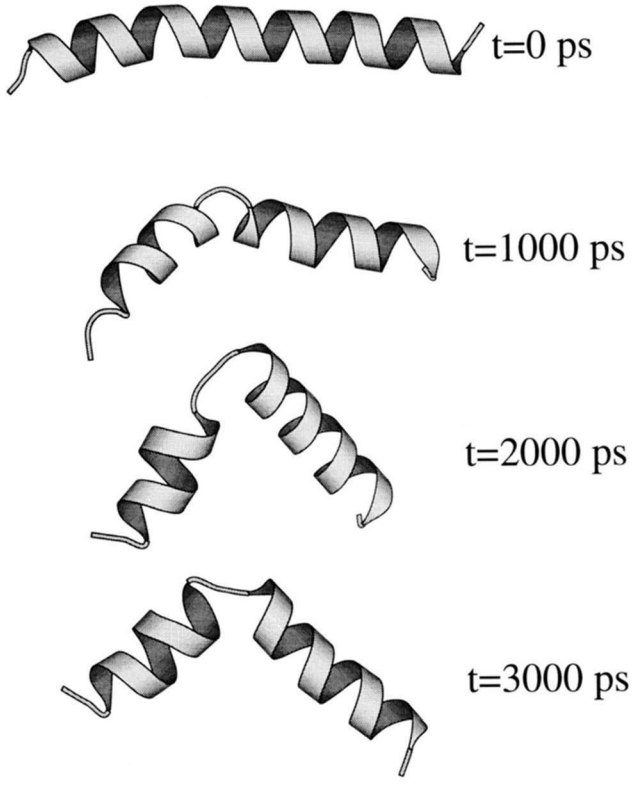

Fig. 3. Snapshots from the MD trajectory of Sim. Pep. Plot was made using MOLSCRIPT (Kraulis, 1991).

The angle between the N-terminal part of the α-helix and the C-terminal part was calculated from the average angle of three vectors in the N-terminal part and three vectors in the C terminus. These vectors were defined by C_α-C_α vectors of $(n, n + 7)$ residues. The 7-residue spacing was used because it corresponds to a rotation over 700 degrees in a perfect α-helix; in this way, our vectors are almost parallel to the helical axis. This procedure gives nine angles at each time step, which were averaged and plotted in Figure 4. The angle is almost 180 degrees, corresponding to a straight α-helix at the start of the simulation, but after 600 ps, it drops quite rapidly to an average value of 90 degrees, with minima below 70 degrees.

RMSD

The RMSD from the crystal structure is a measure of unfolding in peptide simulations. We have calculated the RMSD of the backbone atoms with respect to two different crystal structures (Fig. 5): the starting structure (3CLN, Babu et al., 1988), as well as the structure of CaM complexed with a peptide from MLCK (1CDL, Meador et al., 1992). In the latter crystal structure, the CaM central helix is unfolded in the center (residues Arg 74–Lys 77) and bent around the MLCK peptide. After a sharp rise to more than 0.3 nm (at 250 ps), the RMSD with respect to the starting structure (3CLN) decreases again to 0.08 nm at 510 ps. Then the RMSD rises steadily to 1,400 ps and a plateau value of 0.7 nm is reached. The RMSD with respect to the complexed structure (1CDL) starts at 0.73 nm; it displays a small decrease to 0.63 nm around 250 ps, followed by an increase to 0.7 nm around 500 ps. Then it drops slowly until a minimum of slightly less than 0.3 nm is reached around 1,680 ps. Finally, the RMSD rises to a plateau value of 0.4 nm. The RMSD of the CaM central helix in Sim. Pro with respect to the starting structure (straight) fluctuates between 0.1 and 0.2 nm (data not shown). We have also plotted the RMSD of the C_α atoms of each residue with respect to the starting structure, averaged over the first 500 ps in Sim. Pep and Sim. Pro (Fig. 6). The rationale behind this is that it allows us to see which residues are most flexible in the part of the simulation where the α-helix is still stable. If we disregard the first and last residues, the most flexible region is that from residue Arg 74 through Asp 80 in Sim. Pep. In Sim. Pro, there is only a slight hump in the center of the α-helix. In the same figure, we have added RMS data from a collection of 21 NMR structures of CaM complexed with the CaM-binding domain of MLCK (Ikura et al., 1992). The peak in the RMSD is almost at the same position in the sequence.

Side-chain interactions

Interactions between side chains in the CaM central helix were studied in detail because the large number of charged side chains may be important for the stability of the peptide. We have found

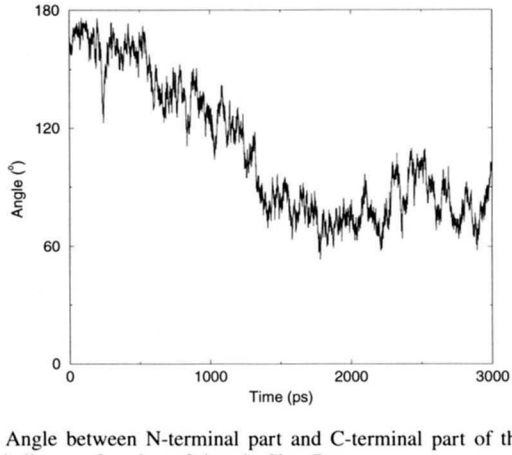

Fig. 4. Angle between N-terminal part and C-terminal part of the CaM central helix as a function of time in Sim. Pep.

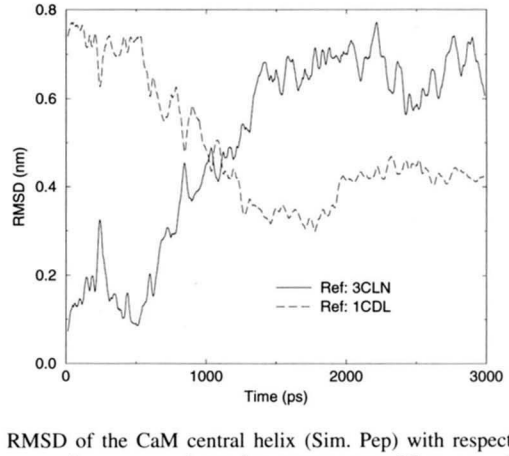

Fig. 5. RMSD of the CaM central helix (Sim. Pep) with respect to two different crystal structures. A running average over 25 ps was plotted to improve clarity.

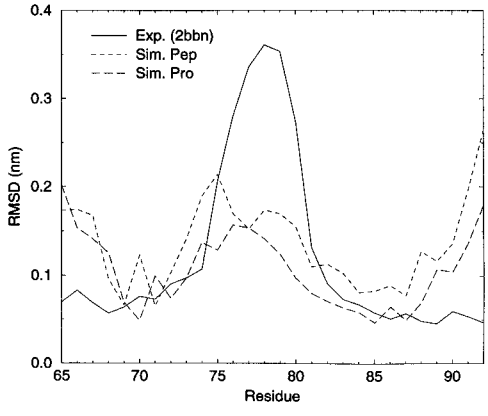

Fig. 6. RMSD of the C_α atoms of the CaM central helix which were averaged per residue over the first 500 ps of the Sim. Pep and the entire Sim. Pro simulations. Also shown is the RMSD for C_α atoms from NMR structure of CaM complexed with peptide from MLCK (Ikura et al., 1992).

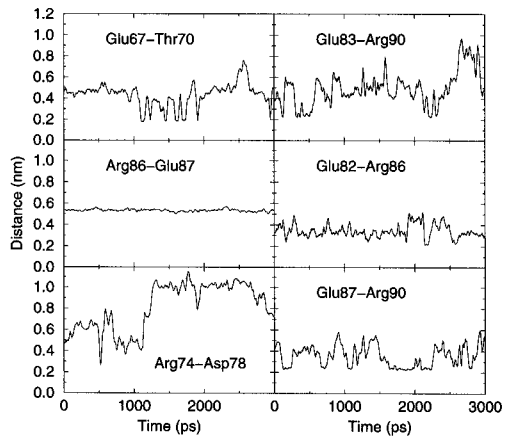

Fig. 8. Distance between attractive side chains, defined as the shortest distance between any atom of both side chains, stabilizing the CaM central helix. A running average over 25 ps was plotted to improve clarity.

that there are helix-stabilizing interactions as well as destabilizing interactions; some of these interactions are present in the crystal structure, others are not. In Figure 7, we have plotted the distance and angle between Phe 65 and Phe 68. It can be seen that the aromatic groups are quite close to each other during the entire simulation (0.59 nm on average); the angle has a two-peaked distribution, around 30 degrees and around 150 degrees. These angles are equivalent because of the symmetry in the Phe residues. The other aromatic pair (Phe 89 and Phe 92) apparently does not interact, the mean distance between the aromatic planes is 0.95 nm (data not shown). Stabilizing salt bridges and hydrogen bonds are present throughout the CaM central helix, especially in the C-terminal part (Fig. 8). Especially important are the interactions between Glu 82 and Arg 86, which are also present in the crystal structure (Babu et al., 1988), and between Glu 87 and Arg 90.

A number of repulsive side-chain combinations are present in the sequence of the CaM central helix at $(n, n + 3)$ and $(n, n + 4)$ positions. We have plotted the distances between these in Figure 9. There are fluctuations in the distance between repulsive side chains of about 0.2 nm, but no larger changes, except for the distance between Arg 74 and Lys 77. The latter changes drastically after 500 ps from 0.6 nm to 1.1 nm. After 1,000 ps, it slowly decreases and, after 1,500 ps, it fluctuates around 0.6 nm. The distance between Arg 86 and Arg 90 is very stable until 2,600 ps when a rather large fluctuation drives the two Arg residues apart. In Figure 10, a number of side chain interactions that can stabilize the bent state have been plotted. There are salt bridges between Arg 74 and Asp 80, Lys 75 and Asp 80, and Arg 74 and Glu 84. Furthermore, a hydrogen bond exists between the Thr 79 alcohol group and the Asp 80 side chain from 780 ps through 2,460 ps (data not shown).

Essential dynamics

The snapshots of the trajectory of the CaM central helix (Fig. 3) in Sim. Pep make it clear that the motion of the peptide is governed by large collective displacements of the individual atoms. This feature makes it interesting to study the peptide by methods that define such collective displacements, such as normal mode anal-

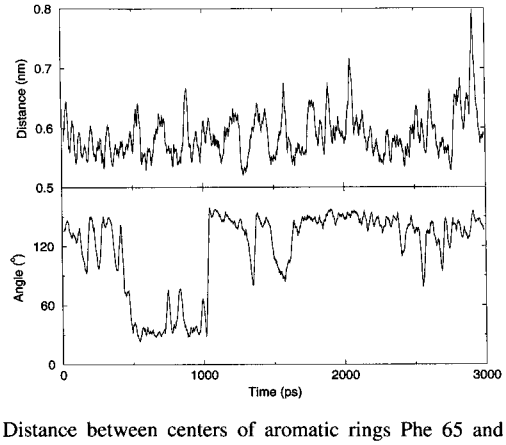

Fig. 7. Distance between centers of aromatic rings Phe 65 and Phe 68 (top), and angle between normal vectors to the plane spanned by CD1, CD2, and CZ atoms of respective residues. A running average over 25 ps was plotted to improve clarity.

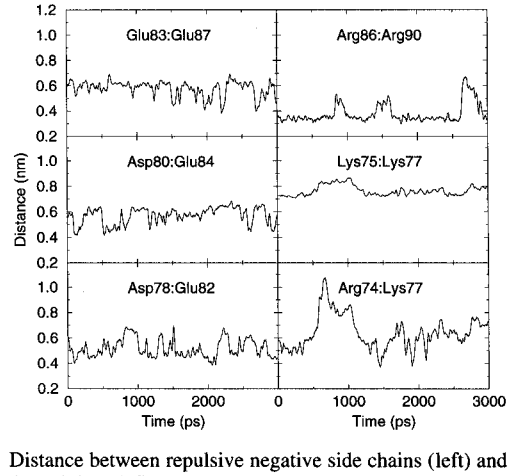

Fig. 9. Distance between repulsive negative side chains (left) and positive side chains (right), defined as the shortest distance between any atom of both side chains. A running average over 25 ps was plotted to improve clarity.

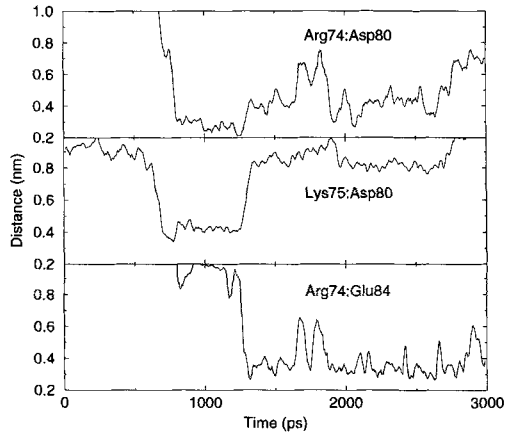

Fig. 10. Distance between side chains that stabilize the bended form by attractive interactions, defined as the shortest distance between any atom of both side chains. A running average over 25 ps was plotted to improve clarity.

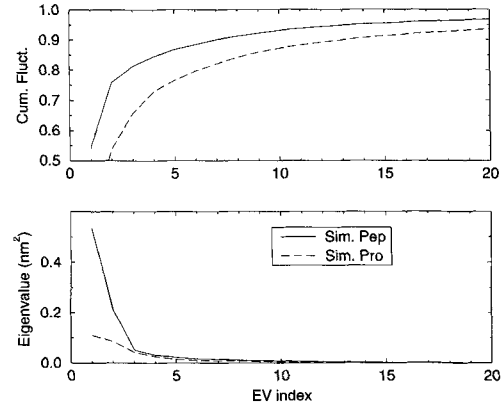

Fig. 11. Eigenvalues (bottom) and cumulative fluctuations (top) as a function of eigenvector index for Sim. Pep and Sim. Pro. Note that only the first 20 of 252 eigenvectors are plotted.

ysis (Brooks & Karplus, 1983; Gō et al., 1983; Levitt et al., 1983) and ED (Amadei et al., 1993) or principal component analysis (Kitao et al., 1991; Hayward & Gō, 1995). Ideally, a large fraction of the total fluctuations in the peptide can be described as a combination of displacements along a small number of vectors, called the essential dynamics (for ED), or normal modes (for NMA). The techniques for this type of analysis have been described in the literature (Case, 1994; Hayward & Gō, 1995) and we will not discuss them here. An ED analysis was performed on the first 500 ps of Sim. Pep and on the integral Sim. Pro trajectories using the ED implementation in the WHAT IF package (Vriend, 1990). Only the backbone atoms (N, C_α, C) were used for the analysis because our prime interest is in the backbone motion. Because there are 84 backbone atoms, there are 252 degrees of freedom. In the case of Sim. Pro, the CaM central helix was cut out of the protein trajectory for this analysis, such that the peptides were the same. For comparison, we also performed an ED analysis on the last 500 ps of Sim. Pep; however, except for a direct comparison of this with the previously mentioned ED analysis of Sim. Pep, we will not discuss this analysis.

The fluctuations along each eigenvector $\mathbf{e}_i$ and the cumulative fluctuations from the eigenvectors ($\mathbf{e}_1$, $\mathbf{e}_2$,... $\mathbf{e}_{3n}$) are plotted in Figure 11. A small number of eigenvectors is sufficient to describe almost all motion in the CaM central helix: the first ten eigenvectors describe 90% of the total fluctuations in Sim. Pep, which is consistent with ED analysis work on proteins (Garcia, 1992; Hayward et al., 1993; van Aalten et al., 1995). This means that we can define an essential subspace spanned by the first ten eigenvectors that covers 90% of the fluctuations of the CaM central helix in Sim. Pep. It can be seen that the first two modes describe a larger part of the fluctuations in Sim. Pep than in Sim. Pro; from $\mathbf{e}_3$ onward, the fluctuations are comparable in both simulations. As a result of this, it takes more eigenvectors to describe an essential subspace that describes 90% of the fluctuations in Sim. Pro (approximately 15).

To characterize the most important eigenvectors of Sim. Pep, we have plotted the structures corresponding to the minimum and maximum displacement along the first three eigenvectors plus the average structure, where the minimum and maximum displacement were taken from the first 500 ps of MD trajectory (Fig. 12). Both $\mathbf{e}_1$ and $\mathbf{e}_2$ correspond to a bending mode, which can be seen from the vibrating string-like deviation from the average structure. In both cases, the wavelength corresponding to the motion seems to be slightly longer than the length of the α-helix. The motion in $\mathbf{e}_3$ is hard to determine from this figure. Another way to characterize the eigenvectors is a component plot (Fig. 13). Each triplet of components of an eigenvector corresponds to the motion of an atom and we have calculated and plotted the length of this vector for each atom. The vibrating string-like deviation from 0 in $\mathbf{e}_1$ can be seen in the component plot, i.e., the atoms around residue 72 and 84 hardly move in this eigenvector, whereas there is a maximum in the amplitude around residue 80, in the center of the α-helix. The motion in $\mathbf{e}_2$ also has the bending property, but superimposed on that is a motion that has a four-residue periodicity along the chain. If we disregard the bending motion in $\mathbf{e}_2$, we see that all residues on one side of the α-helix have similar Cartesian displacements, which indicates that a twisting motion is superimposed on the bending motion. In $\mathbf{e}_3$, we see a standing wave with three nodes at residues 69, 79, and 89.

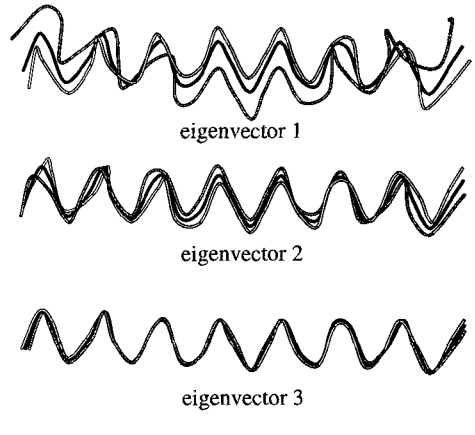

Fig. 12. C_α trace of the CaM central helix for the structures corresponding to the minimum and maximum displacement along the first three eigenvectors of Sim. Pep and the average structure (in black). Plot was made using MOLSCRIPT (Kraulis, 1991).

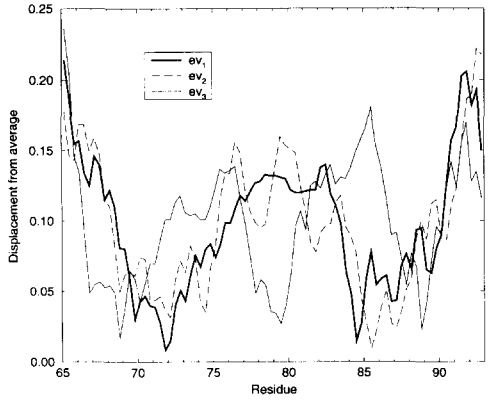

Fig. 13. Atomic components of the first three eigenvectors in Sim. Pep, plotted as the length of the vector defined by the three eigenvector components corresponding to each atom.

To compare the eigenvectors of Sim. Pep with other eigenvectors, we have computed inner products of eigenvector sets. Because the eigenvectors are normalized, an inner product of one means that eigenvectors are identical. In Table 1, we have printed the inner products for the first eigenvectors ($\mathbf{e}_1..\mathbf{e}_4$) of Sim. Pep with the first eigenvectors of the ED analysis of the last 500 ps of Sim. Pep ($\mathbf{e}_1^{end}..\mathbf{e}_4^{end}$), the first eigenvectors of Sim. Pro, the first four normal modes of the CaM central helix (as described below), and the first four eigenvectors from an ED analysis of an experimental data set. The first bending mode ($\mathbf{e}_1$) is still present at the end of the simulation; it corresponds to $\mathbf{e}_1^{end}$. To a large extent, $\mathbf{e}_4^{end}$ is contained in the the first four eigenvectors of Sim. Pep, in particular $\mathbf{e}_2$ and $\mathbf{e}_4$. The correlation between other pairs of vectors is not as pronounced. Between Sim. Pro and Sim. Pep, the first two modes are basically interchanged; when we sum the squares of the inner products for the first two eigenvectors, we find that the similarity is 89%, and the third and fourth eigenvectors of each simulation are very similar as well.

Table 1. *Inner products of eigenvectors between first four EM from Sim. Pep ($\mathbf{e}_i$) and EM from last 500 ps of Sim. Pep ($\mathbf{e}_i^{end}$), EM from Sim. Pro ($\mathbf{e}_i^{pro}$), normal modes ($\mathbf{n}_i'$), and EM from 21 NMR structures ($\mathbf{e}_i^{nmr}$) (Ikura et al., 1992)*[a]

A. EM from last 500 ps of Sim. Pep ($\mathbf{e}_i^{end}$)				
	$\mathbf{e}_1^{end}$	$\mathbf{e}_2^{end}$	$\mathbf{e}_3^{end}$	$\mathbf{e}_4^{end}$
$\mathbf{e}_1$	**0.785**	−0.118	0.063	0.202
$\mathbf{e}_2$	−0.052	0.220	0.072	**−0.602**
$\mathbf{e}_3$	0.023	−0.365	0.015	−0.260
$\mathbf{e}_4$	−0.167	0.055	**0.399**	**0.414**
B. EM from Sim. Pro ($\mathbf{e}_i^{pro}$)				
	$\mathbf{e}_1^{pro}$	$\mathbf{e}_2^{pro}$	$\mathbf{e}_3^{pro}$	$\mathbf{e}_4^{pro}$
$\mathbf{e}_1$	0.410	**0.848**	−0.010	0.028
$\mathbf{e}_2$	**0.852**	**−0.405**	−0.038	−0.044
$\mathbf{e}_3$	−0.074	0.078	**0.714**	**−0.428**
$\mathbf{e}_4$	−0.002	−0.112	0.215	**0.569**
C. Normal modes ($\mathbf{n}_i'$)				
	$\mathbf{n}_1'$	$\mathbf{n}_2'$	$\mathbf{n}_3'$	$\mathbf{n}_4'$
$\mathbf{e}_1$	−0.192	**0.859**	**0.628**	−0.092
$\mathbf{e}_2$	**0.902**	0.321	**−0.508**	−0.054
$\mathbf{e}_3$	−0.026	−0.001	−0.123	**−0.657**
$\mathbf{e}_4$	0.062	−0.035	0.067	**−0.586**
D. EM from 21 NMR structures ($\mathbf{e}_i^{nmr}$)				
	$\mathbf{e}_1^{nmr}$	$\mathbf{e}_2^{nmr}$	$\mathbf{e}_3^{nmr}$	$\mathbf{e}_4^{nmr}$
$\mathbf{e}_1$	0.778	0.062	−0.119	0.033
$\mathbf{e}_2$	−0.180	0.156	−0.282	−0.168
$\mathbf{e}_3$	−0.018	−0.070	−0.052	0.077
$\mathbf{e}_4$	−0.126	0.240	−0.024	−0.023

[a]The most important similarities are marked in bold.

An NMA (Brooks & Karplus, 1983; Gō et al., 1983; Levitt et al., 1983) of the excised CaM central helix was performed as described in Materials and methods. To compare the normal modes to the eigenvectors, we first have to extract the backbone components from the normal modes, and then renormalize the vectors $\mathbf{n}_i$ to a new set of vectors $\mathbf{n}_i'$. This new set is not orthogonal, but projection of a vector $\mathbf{n}_i'$ onto the eigenvectors ($\mathbf{e}_1$, $\mathbf{e}_2$,... $\mathbf{e}_{3n}$) still renders the complete vector back. It can be seen that $\mathbf{n}_1'$ corresponds almost completely to $\mathbf{e}_2$, whereas $\mathbf{n}_2'$ is very similar to $\mathbf{e}_1$. $\mathbf{n}_3'$ is contained in a combination of $\mathbf{e}_1$ and $\mathbf{e}_2$, whereas $\mathbf{n}_4'$ is a combination of $\mathbf{e}_3$ and $\mathbf{e}_4$. It is also possible to construct a set of eigenvectors from experimental structures. For this purpose we used the 21 structures of CaM complexed with the CaM-binding domain of MLCK (Ikura et al., 1992) (pdb entry 2BBN). From these structures, a covariance matrix was built, and the eigenvectors were determined; these eigenvectors then define the difference vectors between the structures. Here we see that there is a clear correspondence between $\mathbf{e}_1$ from Sim. Pep and $\mathbf{e}_1^{nmr}$ from NMR data, but there seems to be no correlation between other pairs of vectors.

Discussion

It is generally thought that CaM can adapt its conformation to enhance binding of different compounds between the two domains, which are connected by the long α-helix. Indeed, it is known that CaM can bind many different proteins or peptides, often inducing α-helical structure in the ligand (Vogel, 1994; Ikura, 1996). From the crystal structure of CaM complexed with a peptide from MLCK (Meador et al., 1992), as well as the NMR structure of a similar complex (Ikura et al., 1992), it is immediately clear that the central helix (residues Phe 65–Phe 92) is flexible in the center, at least from Arg 74 through Glu 83. It should be noted that there are some differences between NMR and X-ray structure that have been attributed to the different composition of the peptide used (Ikura et al., 1992; Meador et al., 1992).

The uncomplexed CaM in aqueous solution, like the complexed CaM, has a flexible region in the central helix. Hydrogen exchange measurements (Spera et al., 1991), NOEs (Ikura et al., 1991), and order parameters (Barbato et al., 1992), as determined by NMR experiments, have shown that the region from Met 76 through Asp 80 is flexible. This region is a subset of the disordered regions found in the complexed structures. It is not hard to imagine that this inherent flexibility facilitates ligand binding: upon complexation, the CaM central helix unrolls as much as necessary to surround the ligand; with its hydrophobic N terminus and hydrophilic C terminus, amphipathic peptides can be accommodated optimally.

The fact that the CaM central helix is a rather regular α-helix in all the plain crystal structures is not too disturbing because the crystals were grown using organic co-solvents, and it has been shown using CD spectroscopy that the α-helix content of CaM increases in solvents that favor the crystallization conditions (Bayley & Martin, 1992).

In this work, we demonstrate that the special properties of the CaM central helix that facilitate complexation with ligands can be reproduced in an MD simulation of the isolated α-helix. This suggests that the flexibility is a property of the CaM central helix only, which is not dependent on, or triggered by the N- and C-terminal domains. In the time span that the α-helix is still stable (the first 500 ps of the simulation), we see that the flexibility is highest in the central region of residues Arg 74–Asp 80 (Fig. 6). After this period, we find that the peptide unfolds, starting with a breaking of the α-helix in the region from Met 76 through Thr 79, around 700 ps. The C-terminal part of the α-helix remains α-helical for the rest of the simulation, whereas the N-terminal part fluctuates between α-helix and π-helix, with, at one instant, as many as 11 residues involved in a π-helix (Fig. 1). Averaged over the whole simulation time, the α-helicity is lowest for residues Met 76–Thr 79 (Fig. 2), consistent with NMR experiments (Spera et al., 1991; Barbato et al., 1992). The dynamic process of bending takes places on a somewhat shorter time scale (500 ps) than the bending motion as determined by NMR relaxation experiments of holo-CaM (Barbato et al., 1992) and apo-CaM (3 ns) (Tjandra et al., 1995). This can probably be explained by the large N- and C-terminal domains of the protein, which will slow bending. Indeed, in Sim. Pro, we find that the amplitude of the bending motions is reduced considerably compared with Sim. Pep. The bending angle of the CaM central helix in Sim. Pep is quite large, it bends from 180 degrees to 70 degrees (Fig. 7). Based on neutron scattering experiments, a "bent" model for CaM in solution was made, in which the angle is about 125 degrees (Heidorn & Trewhella, 1988), which is in between the crystal structure and our data from Sim. Pep. The small angle of 90 degrees, which seems to be the equilibrium angle for the peptide in our simulation, is not possible for the protein because the two domains would overlap. The trajectory of Sim. Pro is not long enough to see a bending motion with a large amplitude, although the ED analysis proves that the bending motion is the most important motion in the simulation. The region of residue Met 76–Thr 79 is also the most flexible region, as determined by the average RMSD in the first 500 ps of the simulation, as well as experimental RMS data (Ikura et al., 1992) (Fig. 6). The RMSD from the starting crystal structure (3CLN, Babu et al., 1988) levels off after 1.3 ns, but at these high values of RMSD, the least-squares fitting procedure is not trivial and RMS is not a very useful criterion for equilibration or stability.

Our side-chain analyses (Figs. 7, 8, 9, 10) show that there are distinctive side-chain interactions stabilizing the N-terminal and the C-terminal end of the CaM central helix in solution. Among these interactions is a salt bridge, Glu 82–Arg 86, that is present in the crystal structure and maintained during the entire simulation (Fig. 8). Another stabilizing interaction is the aromatic interaction between Phe 65 and Phe 68 (Fig. 7). Because this is an $(n, n + 3)$ interaction rather than an $(n, n + 4)$ interaction, the optimal T stacking, well known for aromatic side chains (Burley & Petsko, 1989), is not possible. However, the conformation of the two side chains in our simulation does contribute to the stability of the α-helix. It should be noted that this interaction is not present in the crystal structure; there, the N-terminal end of the α-helix is embedded in the remainder of the protein. In the uncomplexed crystal structures (both in 1CLL, Chattopadhyaya et al., 1992; and 3CLN, Babu et al., 1988), Arg 74 participates in a hydrogen bonding network with residues in the N-terminal domain of the protein; this is also found in computer simulations (Weinstein & Mehler, 1994). In Sim. Pro, we find that Arg 74 interacts with Thr 70 most of the time, and only occasionally with Glu 54, the interaction that prevails in the crystal structure. Because we have a fully solvated protein, it is not surprising that the Arg 74 side chain makes other contacts as well as the crystal contact. In Sim. Pep, interactions with the N-terminal domain are not possible; instead a salt bridge between Arg 74 and Asp 78 forms initially, but it breaks when the helix bends. After 1.3 ns, a very stable salt bridge is formed between Arg 74 and Glu 84, which prohibits restoration of the α-helix. Interestingly removal of residue Glu 84 gives rise to a straightening of the central linker region of CaM in solution (Kataoka et al., 1996). A number of electrostatic interactions seem to be actively destabilizing the central region of the α-helix (Arg 74–Lys 77, Asp 78–Glu 82, Asp 80–Glu 84). There are also some side chains that are not in close proximity initially, that can further stabilize the bended form: Lys 75–Asp 80 and Arg 74–Asp 80 form close contact around 600 ps; after the α-helix is broken, Asp 80 forms a hydrogen bond with Thr 79. A fluctuation in backbone conformation, possibly initiated by the repulsive interactions mentioned above (Fig. 9), makes these contacts possible. It seems that residue Asp 80 is also important for unfolding; it is engaged in repulsive interactions that destabilize the α-helix as well as in attractive interactions that can stabilize the bended form. Furthermore, it is known that aspartate residues are bad α-helix formers in peptides (Chakrabartty & Baldwin, 1995). NMR and CD studies have shown that CaM is more α-helical and has a larger rotation correlation time, indicating a less globular structure, when the pH is decreased (Török et al., 1992). Because a decrease in pH to 4.5 may protonate one or more of the Glu residues in the CaM central helix, this confirms our observation that electrostatic interactions destabilize the CaM central helix.

The ED analysis of the CaM central helix in Sim. Pep shows that the large correlated motions in the CaM central helix involve bending in $\mathbf{e}_1$, a combined twisting and bending in $\mathbf{e}_2$, and a standing wave in $\mathbf{e}_3$ reminiscent of a "first overtone" of $\mathbf{e}_1$ (Fig. 13). Thus, it seems that the CaM central helix behaves somewhat like a string when the α-helix is still formed. When we consider the inner products (Table 1A), it is clear that, at the end of the simulation, $\mathbf{e}_1$ is still important. An extrapolation of $\mathbf{e}_1$, corresponding to a large displacement along $\mathbf{e}_1$, leads to unfolding of the peptide. This motion may be induced by the electrostatic interactions described above. The good correspondence of eigenvectors between Sim. Pep and Sim. Pro (Table 1B) indicates that the simulations are very comparable; they basically span the same essential subspace and hence we can conclude that the simulation of the excised CaM central helix (Sim. Pep) is a good model system for the entire protein, although the amplitudes of the motion are larger in Sim. Pep. We also find that the vectors found by NMA are very similar to the essential modes (Table 1C). Again, we note that normal modes and essential modes span a similar subspace. On the one hand, this may seem surprising, because the deviations from the average structure in the 500-ps simulation are considerable. On the other hand, the most important motions in Sim. Pep resemble vibrating string-like motions, which can be described well by harmonic analysis (Brooks & Karplus, 1983; Gō et al., 1983; Levitt et al., 1983). The frequencies and mode of bending found by the

NMA of the CaM central helix are comparable to those found by Kitao et al. (1991) for melittin. Melittin is a tetramer of identical polypeptide chains consisting of a single α-helix of 26 residues. This α-helix has a Gly residue at position 12 and a Pro residue at position 14, and the most important motion is bending around this region of the peptide; it should be noted that melittin is bent in the crystal structure as well (Terwilliger & Eisenberg, 1982). Although one expects α-helix destabilization when Pro or Gly residues are present in the center of an α-helix, the CaM central helix does not have either of these residues, yet the motions are very similar to those in melittin. Surprisingly, $\mathbf{e}_1$ is also similar to $\mathbf{e}_1^{nmr}$; apparently, the difference between the 21 NMR structures (Ikura et al., 1992) coincides to some extent with displacement in the direction of $\mathbf{e}_1$, i.e., the main difference between these structures is their bending angle around the flexible region of the CaM central helix.

It can be concluded that the simulation of the excised CaM central helix (Sim. Pep) is a good model for the behavior of the α-helix in the intact protein. The location of the bend in Sim. Pep corresponds very well to experimental data from NMR measurements (Spera et al., 1991; Barbato et al., 1992) and the dynamics of the isolated peptide is very similar to that in the intact protein. We emphasize the fact that different theoretical methods (MD/ED and NMA) give consistent results in a relatively complicated system. Recently, Balsera et al. (1996) have argued that an ED analysis does not render a useful essential subspace. However, the test system employed by these authors is G-actin, a 375-residue protein consisting of four subdomains, which is far larger than any of the proteins studied by ED so far (e.g., Garcia, 1992; Amadei et al., 1993; Hayward et al., 1993; van Aalten et al., 1995), whereas their simulation is short (500 ps) compared with their system size. In contrast, we are very confident that our methodology is sound because our results agree very well with experimental results; this confidence is strengthened further by the consistent results from different theoretical methods.

From our results, we can conclude that the unfolding pathway of the CaM central helix is described by an extrapolation of the bending motions in the intact α-helix ($\mathbf{e}_1$ and $\mathbf{e}_2$ from our ED analysis). Although this way of unfolding may be a particular feature of the CaM central helix, the notion that an extrapolation of intrinsic motions may lead to unfolding of α-helices underlies the well-known model for unfolding through a 3_{10}-helix as well (Tirado-Rives & Jorgensen, 1991; Basu et al., 1994).

Materials and methods

Starting structures

The starting structure for our simulation was taken from the crystal structure PDB entry 3CLN (Babu et al., 1988), refined at 2.2 Å. Residues Asp 64–Asp 93 were cut from the protein. Of these, Asp 64 was mutated into an acetyl group by removing the NH group and the side chain, and Asp 93 was mutated into an NH_2 group by removing all atoms beyond the backbone N. This left us with a peptide corresponding to residues Phe 65–Phe 92, with neutral caps on the ends. Sequence characteristics for the peptide are given in Table 2.

Molecular dynamics

The helix was solvated in a cubic box with an edge of approximately 5.0 nm filled with 4,012 SPC (simple point charge) water molecules (Berendsen et al., 1981) for a total of 12,353 atoms. Although the shape of an α-helix would fit in a rectangular box, which would save a large number of water molecules and therefore computer time, our simulations are so long that an α-helix can easily rotate more than 90 degrees, thus allowing the peptide to interact with an image of itself. Therefore, it is necessary to use cubic boxes when simulating α-helical peptides. An energy minimization of the solvated peptide was performed using the steepest descent algorithm for 100 steps. Energy minimization and all simulations were performed using periodic boundary conditions. Then a restrained MD simulation of 20 ps was performed, where the peptide atoms were harmonically restrained to their crystal positions with a force constant of 1,000 kJ mol^{-1} nm^{-2} to allow for further relaxation of the solvent molecules. During the restrained MD run, the temperature was controlled using weak coupling (Berendsen et al., 1984) to a bath of constant temperature (T_0 = 300 K, coupling time τ_T = 0.1 ps) and the pressure was controlled using weak coupling to a bath of constant pressure (P_0 = 1 bar, coupling time τ_P = 0.5 ps). The production run was done with the same pressure- and temperature-coupling constants as the restrained run. Protein and solvent were coupled to the temperature bath separately in restrained as well as free MD. The center of mass motion of the entire simulation system was removed at every step to keep the effective simulation temperature at 300 K. The Gromos-87 forcefield (van Gunsteren & Berendsen, 1987) was used with modifications as suggested in van Buuren et al. (1993); explicit hydrogen atoms were defined in aromatic rings (van der Spoel et al., 1996b; P.M. King, A.E. Mark, & W.F. van Gunsteren, pers. comm.). The time step was 2.0 fs, SHAKE (Ryckaert et al., 1977) was used for all covalent bonds, and a twin-range cut-off criterion for nonbonded interactions was used. The short-range forces (Lennard–Jones and Coulomb) were cut off at 1.0 nm and calculated every step, whereas the long-range forces (Coulomb) were cut off at 1.8 nm and were updated during generation of the neighbor list, which was done every 20 fs.

For the protein simulation, we used the same starting structure as the peptide simulation (3CLN, Babu et al., 1988). All simulation details were the same as the isolated α-helix, except as noted below. A rectangular box of 5.8 × 7.8 × 5.5 nm was used, with 6,768 water molecules, including 69 crystal waters. Four calcium ions from the crystal structure were used, as well as 14 sodium counter ions to make up for the large net charge of −22 on the

Table 2. *Sequence characteristics for the CaM central helix*[a]

Number	6 7 8 9 5678901234567890123456789012
Residue	FPEFLTMMARKMKDTDSEEEIREAFRVF
Structure (3CLN)	HHHHHHHHHHHHHHHHHHHHHHHHHH
id. complexed (1CDL)	HHHHHHHH HHHHHHHHHHHH
Hydrophobic	oo oo ooo o o oo oo
Charge	- ++ +- - --- +- +

[a]Secondary structure was determined by DSSP (Kabsch & Sander, 1983). H, helix; space, no defined secondary structure.

Table 3. *Frequencies corresponding to normal modes of the CaM central helix*

Mode	Frequency (cm^{-1})
1	3.96
2	4.21
3	4.41
4	8.19
5	8.44
6	10.0
7	10.3
8	11.7
9	12.4
10	12.7

protein. A time step of 1 fs was used and SHAKE (Ryckaert et al., 1977) was used for hydrogen atoms only. The length of the simulation was 500 ps. To distinguish both simulations, we have referred to them as "Sim. Pep" and "Sim. Pro." Both simulations were conducted using the GROMACS software package (van der Spoel et al., 1996a) on our custom-built parallel computer (Berendsen et al., 1995) with 32 Intel *i*860 CPUs. The production run for the CaM central helix took 17.3 days on this computer; the protein simulation took 9.7 days.

Normal mode analysis

An NMA (Brooks & Karplus, 1983; Gō et al., 1983; Levitt et al., 1983) of the CaM central helix in Cartesian coordinate space was performed using the implementation in the GROMOS simulation package (van Gunsteren & Berendsen, 1987). We used the GROMOS vacuum force field (van Gunsteren & Berendsen, 1987), rather than the standard force field for solvated biomolecules. In this force field, the charged side-chain groups are replaced by groups with only a dipole. Before the NMA, the structure was energy minimized using the same force field. In a NMA, eigenvectors are determined by diagonalization of the Hessian matrix. Both during energy minimization and the construction of the Hessian, no cut-off for nonbonded interactions was used. The RMSD after minimization with respect to the crystal structure was 0.094 nm. The ten lowest frequencies are given in Table 3.

Acknowledgments

We thank Dr. Andrea Amadei for many stimulating discussions. D.vdS. acknowledges support from the Netherlands Foundation for Chemical Research (SON) with financial aid from the Netherlands Organization for Scientific Research (NWO). H.J.V. acknowledges support from the Medical Research Council (MRC) of Canada and the North Atlantic Treaty Organization (NATO).

References

Amadei A, Linssen ABM, Berendsen HJC. 1993. Essential dynamics of proteins. *Proteins Struct Funct Genet 17*:412–425.

Babu YS, Bugg CE, Cook WJ. 1988. Structure of calmodulin refined at 2.2 Å. *J Mol Biol 204*:191–204.

Balsera MA, Wriggers W, Oono Y, Schulten K. 1996. Principle component analysis and long time protein dynamics. *J Phys Chem 100*:2567–2572.

Barbato G, Ikura M, Kay LE, Pastor RW, Bax A. 1992. Backbone dynamics of calmodulin studied by ^{15}N relaxation using inverse detected NMR spectroscopy: The central helix is flexible. *Biochemistry 31*:5269–5278.

Basu G, Kitao A, Hirata F, Gō N. 1994. A collective motion description of the $3_{10}/\alpha$-helix transition: Implications for a natural reaction coordinate. *J Am Chem Soc 116*:6307–6315.

Bayley PM, Martin SR. 1992. The α-helical content of calmodulin is increased by solution conditions favoring protein crystallization. *Biochim Biophys Acta 1160*:16–21.

Berendsen HJC, Postma JPM, DiNola A, Haak JR. 1984. Molecular dynamics with coupling to an external bath. *J Chem Phys 81*:3684–3690.

Berendsen HJC, Postma JPM, van Gunsteren WF, Hermans J. 1981. Interaction models for water in relation to protein hydration. In: Pullman B, ed. *Intermolecular forces*. Dordrecht: D. Reidel Publishing Company. pp 331–342.

Berendsen HJC, van der Spoel D, van Drunen R. 1995. GROMACS: A message-passing parallel molecular dynamics implementation. *Comp Phys Commun 91*:43–56.

Brooks B, Karplus M. 1983. Harmonic dynamics of proteins: Normal modes and fluctuations in bovine pancreatic trypsin inhibitor. *Proc Natl Acad Sci USA 80*:6571–6575.

Brooks CL III, Case DA. 1993. Simulations of peptide conformational dynamics and thermodynamics. *Chem Rev 93*:2487–2502.

Burley SK, Petsko GA. 1989. Electrostatic interactions in aromatic oligopeptides contribute to protein stability. *Trends Biotech 7*:354–359.

Caflisch A, Karplus M. 1994. Molecular dynamics studies of protein and peptide folding and unfolding. In: Merz KM Jr, Le Grand SM, eds. *The protein folding problem and tertiary structure prediction*. Boston: Birkhaeuser. pp 193–230.

Case DA. 1994. Normal mode analysis of protein dynamics. *Curr Opin Struct Biol 4*:285–290.

Chakrabartty A, Baldwin RL. 1995. Stability of α-helices. *Adv Protein Chem 46*:141–176.

Chattopadhyaya R, Meador WE, Means AR, Quiocho FA. 1992. Calmodulin structure refined at 1.7 Å resolution. *J Mol Biol 228*:1177.

Clore GM, Bax A, Ikura M, Gronenborn AM. 1993. Structure of calmodulin–target peptide complexes. *Curr Opin Struct Biol 3*:838–845.

Daggett V, Levitt M. 1992. Molecular dynamics simulations of helix denaturation. *J Mol Biol 223*:1121–1138.

Finn BE, Forsen S. 1995. The evolving model of calmodulin structure, function and activation. *Structure 3*:7–11.

Garcia AE. 1992. Large-amplitude nonlinear motions in proteins. *Phys Rev Lett 68*:2696–2699.

Gō N, Noguti T, Nishikawa T. 1983. Dynamics of a small globular protein in terms of low-frequency vibrational modes. *Proc Natl Acad Sci USA 80*:3696–3700.

Hayward S, Gō N. 1995. Collective variable description of native protein dynamics. *Annu Rev Phys Chem 46*:223–250.

Hayward S, Kitao A, Hirata F, Gō N. 1993. Effect of solvent on collective motions in globular proteins. *J Mol Biol 234*:1207–1217.

Heidorn DB, Trewhella J. 1988. Comparison of the crystal and solution structures of calmodulin and troponin C. *Biochemistry 27*:909–915.

Hirst JD, Brooks CL III. 1995. Molecular dynamics simulations of isolated helices of myoglobin. *Biochemistry 34*:7614–7621.

Ikura M. 1996. Calcium binding and conformational response in EF-hand proteins. *Trends Biochem 21*:14–17.

Ikura M, Clore GM, Gronenborn AM, Zhu G, Klee CB, Bax A. 1992. Solution structure of a calmodulin–target peptide complex by multidimensional NMR. *Science 256*:632.

Ikura M, Spera S, Barbato G, Kay LE, Krinks M, Bax A. 1991. Secondary structure and side-chain ^{1}H and ^{13}C resonance assignments of calmodulin in solution by heteronuclear multidimensional NMR spectroscopy. *Biochemistry 30*:9216–9228.

Kabsch W, Sander C. 1983. Dictionary of protein secondary structure: Pattern recognition of hydrogen-bonded and geometrical features. *Biopolymers 22*:2577–2637.

Kataoka M, Persechini A, Tokunaga F, Kretsinger RH. 1996. The linker of calmodulin lacking Glu 84 is elongated in solution, although it is bent in the crystal. *Proteins Struct Funct Genet 25*:335–341.

Kazmirski SL, Alonso DOV, Cohen FE, Prusiner SB, Daggett V. 1995. Theoretical studies of sequence effects on the conformational properties of a fragment of the prion protein: Implications for scrapie formation. *Curr Biol 2*:305–315.

Kitao A, Hirata F, Gō N. 1991. The effects of solvent on the conformation and the collective motions of protein: Normal mode analysis and molecular dynamics simulations of mellitin in water and in vacuum. *Chem Phys 158*:447–472.

Kraulis PJ. 1991. MOLSCRIPT: A program to produce both detailed and schematic plots of protein structures. *J Appl Crystallogr 24*:946–950.

Kuboniwa H, Tjandra N, Grzesiek S, Ren H, Klee CB, Bax A. 1995. Solution structure of calcium-free calmodulin. *Nature Struct Biol 2*:768–776.

Levitt M, Sander C, Stern PS. 1983. The normal modes of a protein: Native bovine pancreatic trypsin inhibitor. *Proc Natl Acad Sci USA 10*:181–199.

Meador WE, Means AR, Quiocho FA. 1992. Target enzyme recognition by calmodulin: 2.4 Ångström structure of a calmodulin–peptide complex. *Science 257*:1251.

Mehler EL, Pascual-Ahuir JL, Weinstein H. 1991. Structural dynamics of calmodulin and troponin C. *Protein Eng 4*:625–637.

Persechini A, Kretsinger RH. 1988. The central helix of calmodulin functions as a flexible tether. *J Biol Chem 263*:12175–12178.

Ryckaert JP, Ciccotti G, Berendsen HJC. 1977. Numerical integration of the Cartesian equations of motion of a system with constraints; molecular dynamics of *n*-alkanes. *J Comp Phys 23*:327–341.

Soman KV, Karimi A, Case DA. 1991. Unfolding of an α-helix in water. *Biopolymers 31*:1351–1361.

Spera S, Ikura M, Bax A. 1991. Measurements of the exchange rates of rapidly exchanging amide protons: Application to the study of calmodulin and its complex with a myosin light chain kinase fragment. *J Biomol NMR 1*:155–165.

Terwilliger TC, Eisenberg D. 1982. The structure of melittin. I. Structure determination and partial refinement. *J Biol Chem 257*:6010–6015.

Tirado-Rives J, Jorgensen WL. 1991. Molecular dynamics simulations of the unfolding of an α-helical analogue of ribonuclease A S-peptide in water. *Biochemistry 30*:3864–3871.

Tjandra N, Kuboniwa H, Ren H, Bax A. 1995. Rotational dynamics of calcium-free calmodulin studied by ^{15}N-NMR relaxation measurements. *Eur J Biochem 230*:1014–1024.

Török K, Lane AN, Martin SR, Janot JM, Bayley PM. 1992. Effects of calcium binding on the internal dynamics properties of bovine brain calmodulin studied by NMR and optical spectroscopy. *Biochemistry 31*:3452–3462.

van Aalten DMF, Amadei A, Linssen ABM, Eijsink VGH, Berendsen HJC. 1995. The essential dynamics of thermolysin: Confirmation of the hinge-bending motion and comparison of simulations in vacuum and water. *Proteins Struct Funct Genet 22*:45–54.

van Buuren AR, Berendsen HJC. 1993. Molecular dynamics simulation of the stability of a 22-residue alpha-helix in water and 30% trifluoroethanol. *Biopolymers 33*:1159–1166.

van Buuren AR, Marrink SJ, Berendsen HJC. 1993. A molecular dynamics study of the decane/water interface. *J Phys Chem 97*:9206–9212.

van der Spoel D, van Buuren AR, Apol E, Meulenhoff PJ, Tieleman DP, Sijbers ALTM, van Drunen R, Berendsen HJC. 1996a. *Gromacs user manual, version 1.3*. Nijenborgh 4, 9747 AG Groningen, The Netherlands. Internet: http://rugmd0.chem.rug.nl/~gmx.

van der Spoel D, van Buuren AR, Tieleman DP, Berendsen HJC. 1996b. Molecular dynamics simulations of peptides from BPTI: A closer look at amide–aromatic interactions. *J Biomol NMR*. Forthcoming.

van der Spoel D, Vogel HJ, Berendsen HJC. 1996c. Molecular dynamics simulations of N-terminal peptides from a nucleotide binding protein. *Proteins Struct Funct Genet 24*:450–466.

van Gunsteren WF, Berendsen HJC. 1987. *Gromos-87 manual*. Biomos BV, Nijenborgh 4, 9747 AG Groningen, The Netherlands.

Vogel HJ. 1994. Calmodulin: A versatile calcium mediator protein. *Biochem Cell Biol 72*:357–376.

Vogel HJ, Zhang M. 1995. Protein engineering and NMR studies of calmodulin. *Mol Cell Biochem 149/150*:3–15.

Vorherr T, Kessler O, Mark A, Carafoli E. 1992. Construction and molecular dynamics simulation of calmodulin in the extended and in a bent conformation. *Eur J Biochem 204*:931–937.

Vriend G. 1990. WHAT IF: A molecular modeling and drug design program. *J Mol Graphics 8*:52–56.

Weinstein H, Mehler EL. 1994. Ca^{2+}-binding and structural dynamics in the functions of calmodulin. *Annu Rev Physiol 56*:213–236.

Zhang M, Tanaka T, Ikura M. 1995. Calcium-induced conformational transition revealed by the solution structure of apo calmodulin. *Nature Struct Biol 2*:758–767.

Zhang M, Vogel HJ. 1994. Two dimensional NMR studies of selenomethionine calmodulin. *J Mol Biol 234*:545–554.